PERGAMON

Deep-Sea Research II 49 (2002) 4355–4367

DEEP-SEA RESEARCH
PART II

www.elsevier.com/locate/dsr2

Air–sea CO_2 fluxes on the US Middle Atlantic Bight

M.D. DeGrandpre[a,*], G.J. Olbu[a], C.M. Beatty[a], T.R. Hammar[b]

[a] *Department of Chemistry, The University of Montana, 32 Campus Dr., Missoula, MT 59812, USA*
[b] *Department of Applied Physics and Engineering, Woods Hole Oceanographic Institution, Woods Hole, MA 02543, USA*

Accepted 12 February 2002

Abstract

One objective of the Ocean Margins Program (OMP) was to quantify air–sea CO_2 fluxes on the US Middle Atlantic Bight (MAB). No measurements of the partial pressure of CO_2 (pCO_2) had been reported for the MAB prior to the 1994 OMP field program. A number of field studies have now taken place that include ship and mooring-based measurements of pCO_2 spanning the years 1994–2000. We use these data to quantify the annual air–sea CO_2 flux on the MAB. These calculations indicate that the MAB is a net annual sink for atmospheric CO_2, with the inner, mid, and outer-shelf regions taking up $\sim$0.1, 0.7, and 0.2 Mt C yr^{-1}, respectively, for a net uptake of $\sim 1 \pm 0.6$ Mt C yr^{-1}. The annual cycle of heating and cooling combined with high winds during the period of undersaturation (winter) appear to account for a significant portion of the uptake. The flux uncertainty is dominated by uncertainty of the gas-transfer velocity parameterization, atmospheric CO_2 levels, and coarse spatial pCO_2 resolution. Errors due to monthly averaging of wind and pCO_2 time-series are relatively small in comparison. Recent results from other ocean margin regions found a significantly larger flux (in mol m^{-2} yr^{-1}). Unlike the MAB, the increase in pCO_2 due to summer heating appears to be counterbalanced by new production and the pCO_2 never rises significantly above atmospheric saturation in these areas.

1. Introduction

Many studies have focused on quantifying the various sources and sinks of the global carbon cycle. Major oceanographic field studies have set out to quantify the uptake of anthropogenic CO_2 in both ocean basins and margins. For a variety of logistical and political reasons, carbon fluxes have been quantified in few ocean margins (Liu et al., 2000a). Ocean margins sustain a high level of biological productivity as a result of the large influx of riverine, estuarine, and offshore nutrients. The high rates of primary production efficiently reprocess incoming inorganic and organic carbon, generating new organic carbon (Smith and Hollibaugh, 1993). If the carbon in its various forms is buried in sediments or exported to the open-ocean prior to release as CO_2, margins can be significant sinks of atmospheric CO_2 (Tsunogai et al., 1999; Wang et al., 2000; Frankignoulle and Borges, 2001). (To be a sink of atmospheric CO_2 does not imply storage of the carbon in the margin but simply a net flux into the ocean from the atmosphere.) Temporal and spatial mapping of the air–sea CO_2 gradient (ΔpCO_2) is the most straightforward approach to determine if a margin is an atmospheric source or sink. Surface pCO_2

*Corresponding author. Tel.: +1-406-243-4118; fax: +1-406-243-4227.
E-mail address: mdegrand@selway.umt.edu (M.D. DeGrandpre).

0967-0645/02/$ - see front matter
PII: S0967-0645(02)00122-4

measurements, perfected only over the past ~20 years, have primarily been made in open-ocean areas where fluxes are expected to be much larger relative to continental margins simply due to the larger surface area. These flux studies are time-intensive because they are only meaningful, from a global perspective, if annual fluxes can be determined. Although open-ocean regions have been the focus, few areas have been visited frequently enough to resolve the annual cycle, e.g., >4 times per year. Even less is known about the annual pCO_2 cycle in most ocean margins.

Surface pCO_2 data collected over month to year-long periods have been reported for a few ocean margins including the Bering Sea (Codispoti et al., 1982), North Sea (Kempe and Pegler, 1991; Hoppema, 1991), Northeastern Atlantic shelf (Frankignoulle and Borges, 2001), Middle Atlantic Bight (Boehme et al., 1998), and East China Sea (Tsunogai et al., 1999; Wang et al., 2000). (In this discussion only continental shelf areas of ocean margins are considered, estuaries and enclosed seas are excluded.) The East China Sea and Northeastern Atlantic shelf have been more intensively studied providing the first estimates of annual continental margin air–sea CO_2 flux (Tsunogai et al., 1999; Wang et al., 2000; Liu et al., 2000a; Frankignoulle and Borges, 2001). Both are net CO_2 sinks with fluxes of −2.9 (W) (East China) and −2.8 (W) (Northeastern Atlantic shelf) mol C m^{-2} yr^{-1}. For comparison, the fluxes in the Northeastern Pacific Ocean (Wong and Chan, 1990) and North Atlantic Ocean near Bermuda (Bates et al., 1996) are −0.7 (LM) and −0.6 (T) mol C m^{-2} yr^{-1}, respectively. The fluxes were calculated from the Liss and Merlivat (1986) (LM), Wanninkhof (1992) (W) or Tans et al. (1990) (T) gas-transfer parameterizations. Tsunogai et al. (1999) speculated that if all continental margins had fluxes similar to the East China Sea, total margin fluxes could be as high as 1 Gt C yr^{-1}, comparable to open-ocean fluxes (~2 Gt C yr^{-1}).

For a margin to be a net sink of atmospheric CO_2, it must overcome a number of processes that can act to increase surface seawater pCO_2. Large amounts of terrestrial organic carbon flow into continental margins, and if the residence time of the organic-rich water is significant, much of the organic carbon may be remineralized on the shelf, increasing surface pCO_2. Uptake of nutrients from freshwater or atmospheric sources will counteract remineralization to some extent. Coastal upwelling increases pCO_2 by returning CO_2-rich water to the surface. If the CO_2 is not rapidly drawn down by utilization of the accompanying nutrients, upwelling can lead to sustained supersaturation. Furthermore, if the organic matter produced is remineralized before burial or export to deeper waters, the upwelled CO_2 will be eventually lost to the atmosphere. Benthic fluxes and formation of particulate inorganic carbon (PIC) also may increase sea surface pCO_2 in some areas (Liu et al., 2000b). Many margins also experience significant summer heating which drives pCO_2 upward. Whether a margin is a source or sink ultimately depends upon rates of ingassing, organic carbon production, burial, water export and cooling being large relative to rates of offgassing, organic remineralization, PIC formation, and heating. In the East China Sea, net cooling and biological production leads to CO_2 undersaturation (Tsunogai et al., 1999). The cold, dense water flows offshore, efficiently exporting organic and remineralized carbon before it can be returned to the atmosphere by offgassing. Similar mechanisms appear to be at work in other ocean margins (e.g., Frankignoulle and Borges, 2001).

In the present paper we use a number of existing surface pCO_2 data sets to quantify the air–sea CO_2 flux on the MAB. We also present a qualitative interpretation of the pCO_2 seasonal and spatial trends and resulting flux; a general interpretation of inorganic carbon cycling on the MAB is beyond the scope of the present manuscript.

2. Methods

2.1. pCO_2 measurements

Both ship- and mooring-based pCO_2 measurements have been made on the MAB since 1993. The shipboard data include those of Chipman et al. (1995), Takahashi et al. (2001) and Boehme et al. (1998). An underway pCO_2 NDIR-equilibrator system was used for the Chipman et al. (1995) and

Takahashi et al. (2001) measurements as described in Bates et al. (1998). The uncertainty in these measurements is estimated to be $\pm 1.5\,\mu$atm ([7]Chipman et al., 1995). The Boehme et al. (1998) pCO_2 data were calculated from total alkalinity and total CO_2 measured on discrete samples. They estimate the uncertainty to be $\pm 6\,\mu$atm. Mooring-based pCO_2 measurements were obtained at various locations on the MAB. These measurements were performed using an autonomous, in situ pCO_2 system (SAMI-CO_2) (DeGrandpre et al. 1995, 1997, 1999). The calibration procedures are described in detail in DeGrandpre et al. (1995, 1999). All in situ measurements were performed at half-hour intervals. Shipboard data were used to verify the accuracy of the in situ data. All shipboard data were adjusted to the in situ temperature. Ship and mooring data agreed to within $\pm 10\,\mu$atm. There were typically 2–3 intercalibration measurements for each deployment period. Since the ships rarely approached the moorings closer than 1 km, some of the uncertainty arose from water mass differences between the mooring and ship. All data are reported as wet pCO_2, i.e. saturation with water vapor, corrected to the local barometric pressure. All temporal and spatial data were interpolated on 1 h and 1 km intervals, respectively.

We explored expanding the data coverage by predicting pCO_2 through multiple linear regression techniques, similar to that presented in Tsunogai et al. (1999). Parameters derived from dissolved O_2, salinity, and temperature could not predict sea-surface pCO_2 to better than ± 25–$50\,\mu$atm. Because of this large uncertainty and the availability of a relatively extensive data set collected during and since the OMP, we chose to rely strictly on directly measured or carbonate-parameter derived pCO_2.

2.2. Gas flux calculations

Air–sea gas fluxes are calculated using the diffusive boundary layer model:

$$F = K_w S\,\Delta pCO_2, \tag{2.1}$$

where F is the gas flux (e.g. in mol C m^{-2} yr^{-1}), K_w is the gas-transfer velocity, S is CO_2 solubility (Weiss, 1974), and ΔpCO_2 is the partial pressure difference between the sea-surface and atmosphere. The gas-transfer velocity is controlled by sea-surface turbulence and bubble injection, but since these parameters are not easily measured, it is commonly estimated using empirically derived relationships based on wind speed. We use two relationships derived from field and laboratory studies (Liss and Merlivat, 1986; Wanninkhof, 1992) in order to provide bounds on the uncertainty in the flux due to uncertainty in K_w. The Liss and Merlivat (1986) relationship estimates lower K_w's than Wanninkhof (1992) for the same wind speed, especially at intermediate (3–6 m s^{-1}) wind speeds. Gas-transfer velocities have been directly measured on the MAB at Georges Bank (Wanninkhof et al., 1993). Their deliberate tracer experiment found K_w's close to those predicted by the Wanninkhof (1992) relationship. Wallace and Wirick (1992) previously found very high gas-transfer velocities for dissolved oxygen on the MAB, with a strong dependence on significant wave height and orbital wave velocities. Dissolved O_2 time-series data obtained during the OMP did not show similar rapid changes in DO saturation; therefore we chose not to use the relationship derived from that study. Gas-transfer velocities were calculated using winds obtained from NOAA NDBC buoys (Fig. 1). NDBC sea-surface temperatures or SAMI in situ temperatures were used for calculation of S and K_w.

Atmospheric CO_2 also enters into the flux calculation. Continental CO_2 sources may increase atmospheric pCO_2 over the MAB. Boehme et al. (1998) found a mean atmospheric mole fraction (xCO_2) of 377 ppm from 1994 to 1996. Farther offshore, the measurements of Chipman et al. (1995) recorded levels closer to clean marine air (360 ppm). Our measurements of atmospheric CO_2 using an automated NDIR-based system on Duck pier, NC (~ 0.5 km offshore) for 43 d during autumn 1996 found a mean xCO_2 of 366 ± 6 ppm ($N = 1817$). An atmospheric mole fraction of 360 ppm was used for the flux calculations here. The xCO_2 was converted to partial pressure by assuming 100% humidity and using the mean barometric pressure from NOAA NDBC buoys.

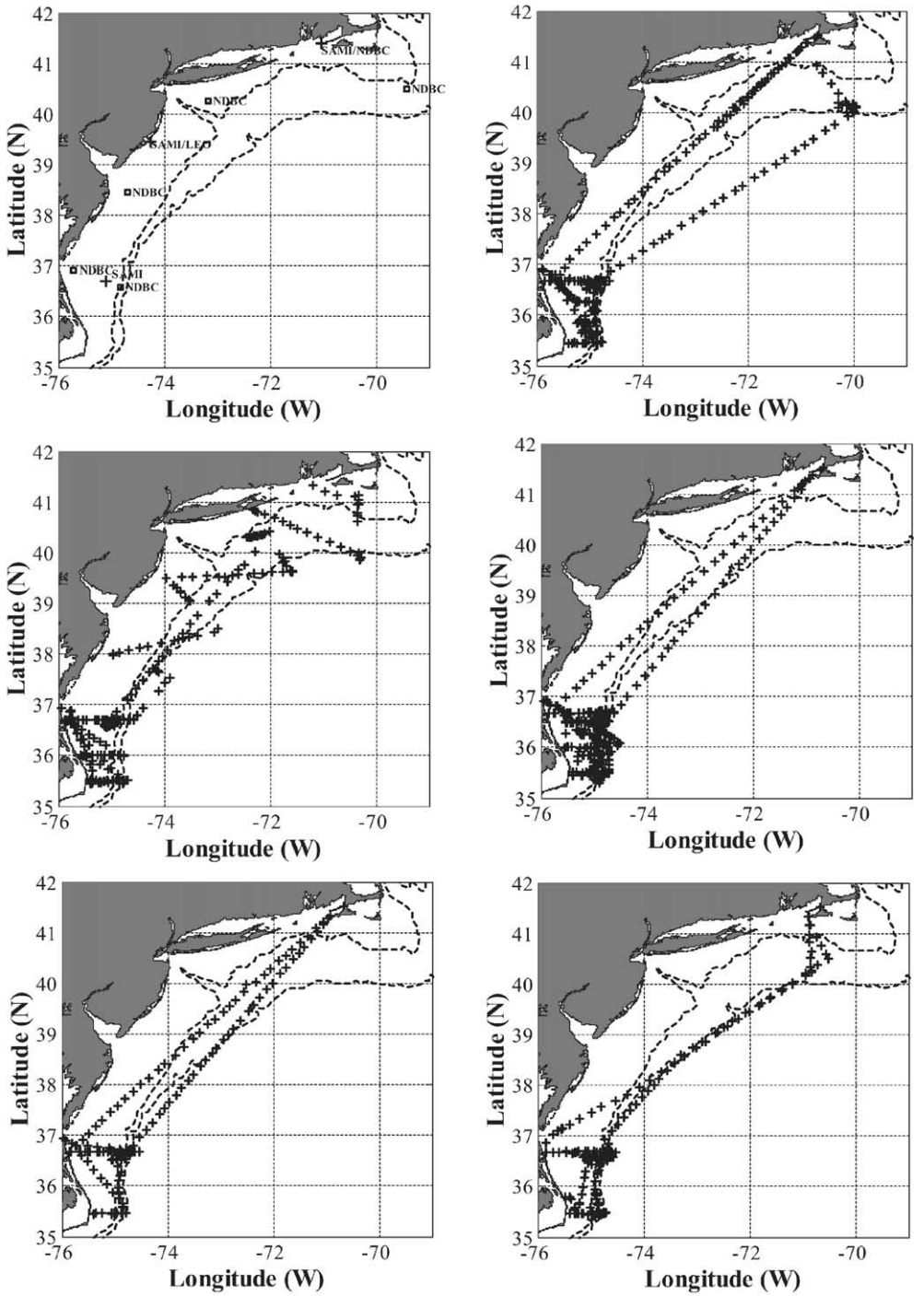

Fig. 1. Maps of the US Middle Atlantic Bight showing the 50 and 200 m isobaths which define the outer borders of the mid and outer shelves. The 20 m isobath, delineating the inner-shelf, is very near shore and is omitted for clarity. Locations of the SAMI moorings, NDBC buoys, and LEO line are shown in the upper left. The five pCO_2 cruises performed by Chipman et al. (1995) and Takahashi et al. (2001) utilized in the manuscript are shown. The + 's represent transects performed during February, March, May, June and October 1996, going from left to right starting from upper right. The cruise track used to estimate fluxes on the outer-shelf extends from Woods Hole, MA to Cape Hatteras and transects the outer-shelf (50–200 m).

2.3. Data sets

Cruises between 1993 and 1996 reported by Chipman et al. (1995) and Takahashi et al. (2001) mapped sea-surface pCO_2 over significant portions of the MAB (Fig. 1). Cruise dates are given in the Fig. 1 caption. Boehme et al. (1998) performed monthly cross-shelf transects off New Jersey (LEO-line) between 1994 and 1996. Mooring-based pCO_2 measurements (DeGrandpre, unpublished) were obtained off Cape Hatteras during 1996 (36.69°N, 75.10°W), on the 15 m isobath off New Jersey (LEO-15) (39.46°N, 74.26°W) during periods between 1997 and 2000, and on the 20 m isobath in Buzzards Bay (BB) (41.40°N, 71.03°W) during 1999–2000 (Fig. 1). The coverage of ship transects and locations of pCO_2 moorings are shown in Fig. 1. Hereafter, the three data sources are referred to as CHIP (Chipman et al., data), LEO (Boehme et al., data), and SAMI (DeGrandpre et al., data). The MAB is defined to be all water shoreward of the 200 m isobath (Fig. 1). Based on the spatial variability found by Boehme et al. (1998) and in this study, we define the inner, mid, and outer-shelf as water between 0–20, 21–50, and 51–200 m isobaths, respectively. Almost no data exist for the Georges Bank area east of Cape Cod; therefore, the fluxes reported here apply only to waters between Cape Cod and Cape Hatteras.

We utilize the available ship and mooring-based pCO_2 data sets to estimate the mean seasonal ΔpCO_2 for different regions of the MAB. The regional fluxes are used to calculate the annual flux over the MAB. We first examine spatial and temporal scales of variability to determine if a limited data set can be used to describe this relatively complex oceanographic regime. Uncertainty due to K_w formulations, different averaging of the ΔpCO_2 and wind, and the atmospheric pCO_2 are also assessed.

3. Results

3.1. Spatial and temporal scales of variability

Ideally, shipboard mapping would have provided sufficient spatial and temporal coverage to accurately estimate the regional ΔpCO_2; however, as can be seen in Fig. 1, spatial and seasonal coverage was limited. For this reason, we utilize a combination of CHIP, LEO, and SAMI data to determine spatial and temporal scales of variability. As presented below, SAMI and LEO data are used to estimate inner and mid-shelf fluxes. Outer-shelf fluxes are estimated using CHIP data, more specifically, five cruise tracks between Woods Hole, MA, and Cape Hatteras that transected the outer-shelf during 1996 (Fig. 1).

3.2. Inner-shelf

Boehme et al. (1998) found that surface pCO_2 was highly variable nearshore (<20 m depth) and that their monthly cruises did not adequately resolve the temporal variability. Surface pCO_2 could range from <300 μatm to >600 μatm from one cruise to the next. The SAMI data are the only other inner-shelf data available, and they confirm the highly dynamic nature of pCO_2 in these waters (Fig. 2). Although the Buzzards Bay and LEO sites are separated by ~ 300 km and the data were collected during two different years, the two time-series are remarkably similar both in magnitude and long-term trend. Surface pCO_2 peaks in the summer but is highly variable, swinging from 10 to 100s of μatm above and below atmospheric saturation over very short time periods. The variability and overall magnitude declines during autumn, and both reach a minimum during winter. These seasonal trends are confirmed by the nearshore LEO time-series data (also shown in Fig. 2). Local freshwater input and upwelling are probably the primary sources of the large short-term changes on the inner-shelf (Boehme et al., 1998; Glenn et al., 1996). The short-term fluctuations are overlaid on mesoscale forcings such as high-latitude freshwater input (Loder et al., 1998), seasonal heating and cooling, and intrusion of slope waters (Aikman, 1984; Biscaye et al., 1994).

The mean seasonal inner-shelf ΔpCO_2's are compared in Table 1. Not surprisingly there is considerable variability between the different years and locations. The limited temporal resolution of the LEO data significantly increases the uncertainty for these ΔpCO_2's, and we therefore do not

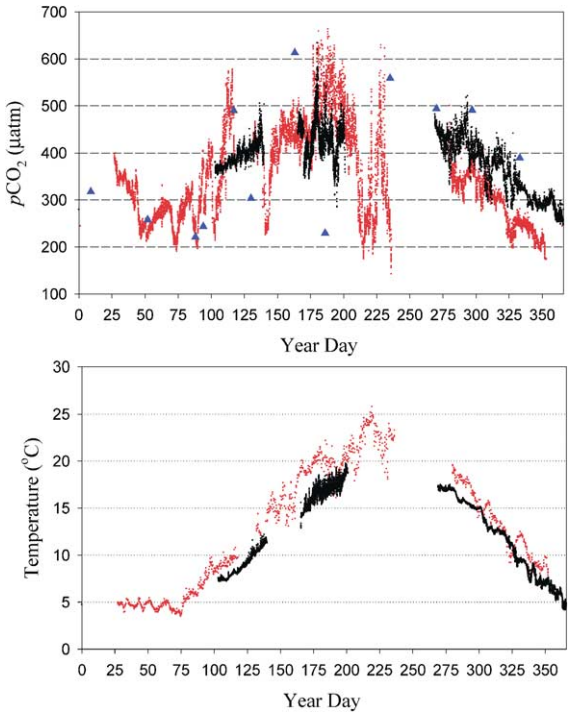

Fig. 2. SAMI mooring pCO_2 and temperature time-series from Buzzards Bay (black dots) and LEO-15 (red dots). Also shown are the inner-shelf LEO pCO_2 data collected by Boehme et al. (1998) (blue triangles). Locations are shown in Fig. 1.

use these data for flux calculations. However, the similar trends and magnitude of the SAMI data between the two mooring sites suggest that alongshore gradients are small. We therefore assume that the two data sets are representative of the entire MAB inner-shelf ΔpCO_2. As presented below, distributions in the mid-shelf region also support that alongshore variability is small. To estimate the inner-shelf flux, we hourly interpolated each mooring ΔpCO_2 over the annual cycle, calculated the hourly flux for each location, and averaged the two results. The uncertainty is propagated through the calculations to account for the inner-shelf contribution to the uncertainty of the overall MAB flux (see below).

3.3. Mid-shelf

The LEO data set is used to quantify fluxes in the mid-shelf region. Both CHIP and SAMI data were obtained only over limited time periods, but they are useful to evaluate if the LEO data are characteristic of the entire MAB. Based on a comparison between SAMI and LEO 1996 data, we argued that surface pCO_2 levels are very similar in the alongshore direction over most of

Table 1
Mean seasonal ΔpCO_2 calculated for different data sets collected on the MAB between 1994 and 2000

	Location	Seasonal Mean ΔpCO_2 (µatm)			
		Jan–Mar	Apr–May	Jun–Aug	Sept–Dec
Inner-shelf	SAMI BB (2000)	−35	+61	+63	0
	SAMI LEO-15 (1999)	−66	+49	+15	−65
	LEO (1994–1995)	−90	+24	+80	+53
Mid-shelf	LEO (1994–1995)	−81	−16	+49	−29
	CHIP (1996)	−87[a]	+8[b]	nd	nd
	SAMI Cape Hatteras (1996)	−70	nd	nd	nd
Outer-shelf (1996)	CHIP[c] (1996)	−31	−6	+20	−14
	CHIP[a] (1996)	−35	nd	nd	nd

To insure equal weighting within each data set, means from time-series were calculated using hourly interpolated data while means from transects were calculated using data interpolated over 1 km intervals. Buzzards Bay (BB) and LEO-15 data are SAMI mooring data while LEO are ship-based data collected by Boehme et al. (1998). CHIP data were collected by Chipman et al. (1995) and Takahashi et al. (2001).

nd = no data.

[a] Cross-shelf transects over entire MAB.

[b] Single cross-shelf transect.

[c] 5 alongshore transects.

the mid-shelf MAB (DeGrandpre and Reimers, 2000). The two locations, both on the 30 m isobath but separated by ~280 km, had similar pCO_2 levels and trends during the 90-d mooring deployment period (Fig. 3). The mean ΔpCO_2 for the hourly interpolated LEO and SAMI data averaged over the same 90-d period were −81 and −70 μatm, respectively (Table 1). Transect data obtained during March 1996 also support that pCO_2 levels are very similar in the alongshore direction. The mean ΔpCO_2 CHIP data for the five mid-shelf transects during the March 1996 cruise were –87 μatm (Table 1). Except for the northern transect, mid-shelf surface pCO_2 ranged from ~210 to 250 μatm, with a mean of 241 ± 22 μatm. The northern, high pCO_2, transects were associated with cold water, suggesting that upwelling was influencing pCO_2 levels in this region. The other period when CHIP data were collected in the northern mid-shelf indicate that high pCO_2 levels

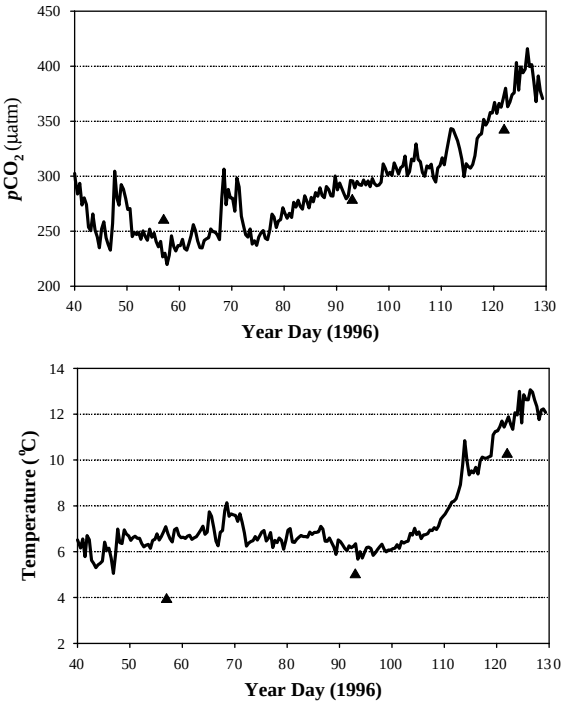

Fig. 3. SAMI mooring pCO_2 and temperature time-series at Cape Hatteras (solid line) along with the LEO data (black triangles), both collected in 1996 on the ~30 m isobath. Locations are shown in Fig. 1.

are not a persistent feature (mean ΔpCO_2 was +8 μatm during May 1996).

Others have found that surface biogeochemical gradients are small alongshore on the central MAB. Sharp and Church (1981) collected seasonal nutrient data and found homogeneous concentrations over their 150 km alongshore transect. Surface dissolved oxygen (Falkowski et al., 1988), chl *a* concentrations (Ryan et al., 1999) and rates of primary production (O'Reilly and Busch, 1984) also have been observed to have little alongshore variability. As expected, alongshore hydrography also follows these patterns (Falkowski et al., 1983; Münchow and Garvine, 1993). In fact, strong cross-shelf gradients and weak alongshore gradients are common features of coastal margins (e.g., Tsunogai et al., 1999; Kempe and Pegler, 1991), largely due to freshwater-generated cross-shelf density gradients and buoyancy-driven alongshore flow (Aikman, 1984; Münchow and Garvine, 1993). Similar pCO_2 patterns, weak alongshore and large cross-shelf gradients, are characteristic of the East China Sea (Tsunogai et al., 1999).

Because of the similarities in ΔpCO_2 determined from the SAMI, LEO and CHIP (March 1996) data, we assume that the LEO data, which were obtained over multiple years (Boehme et al., 1998), represent the mid-shelf ΔpCO_2 for the entire MAB. The LEO data, averaged between the ~20 and 30 m isobaths, are interpolated hourly for the flux calculations. The uncertainty is assessed by comparison with the ΔpCO_2 estimated using the CHIP and SAMI data during seasons when they were available (Table 1). The uncertainty is calculated from the mean ΔpCO_2 and is then propagated through the remaining calculations (see below).

3.4. Outer-shelf

The outer-shelf data are comprised of five Cape Cod to Cape Hatteras alongshore transects performed in 1996 (Figs. 1 and 4) and the outer portion of the cross-shelf transects in March 1996. The mean ΔpCO_2's are shown in Table 1, averaged over the entire transect for each period. Transects were averaged together if more than one cruise took place during one period, i.e. January–March and April–June (Fig. 1). The alongshelf transect in

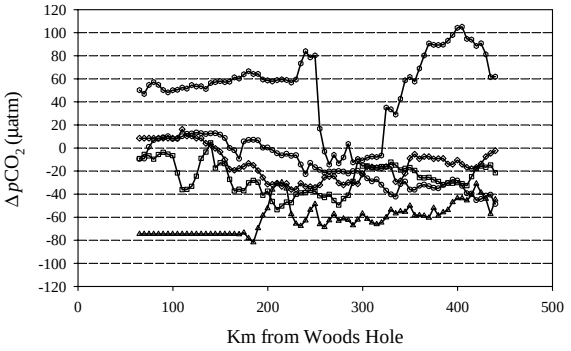

Fig. 4. The interpolated ΔpCO_2 along the outer-shelf Cape Cod to Cape Hatteras transects. The data correspond to transects during February (○), March (△), May (□), June (⬡), and October (◇) in 1996 as shown in Fig. 1.

March 1996 closely compares to the mean ΔpCO_2 estimated from the outer-shelf cross-shelf transects performed during that cruise (Table 1). Fronts, associated with changes in temperature and salinity (data not shown), are clearly evident in the transects, especially during the June cruise. The frontal features reflect the complex oceanography of the outer-shelf. The shelf-slope front is a distinct hydrographic feature in this region (Aikman, 1984) and is accompanied by large biogeochemical gradients (Falkowski et al., 1988; Wirick, 1994; Vodacek et al., 1997). Intrusion of the Gulf Stream onto the outer-shelf is also common, especially in the southern MAB (Churchill and Cornillon, 1991).

For calculation of the outer-shelf flux, each transect was interpolated over 1 km intervals and an average ΔpCO_2 was calculated for each of the five different time periods. From these spatially averaged ΔpCO_2's, an hourly interpolated ΔpCO_2 was generated over the annual cycle. In this case, only the CHIP cross-shelf transects obtained during March 1996 are available to evaluate the uncertainty in the outer-shelf flux.

4. Discussion

4.1. General patterns

The annual cycles of surface pCO_2 for the three shelf regions are shown in Fig. 5. The entire shelf is significantly undersaturated during the winter

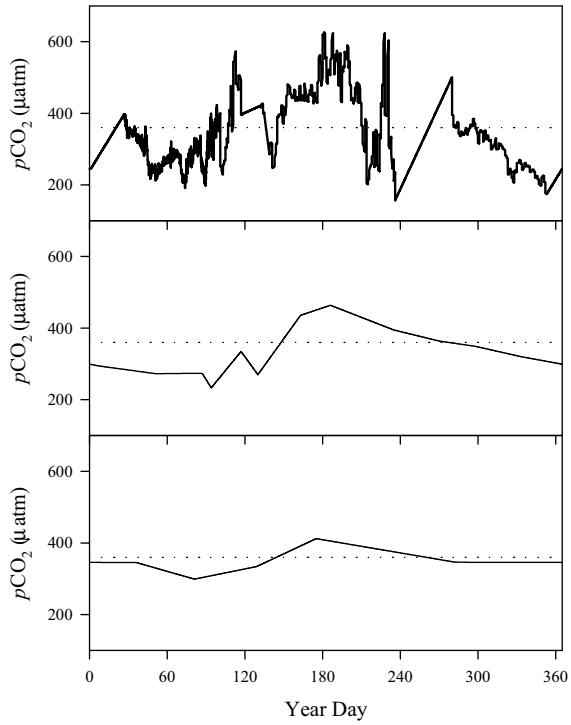

Fig. 5. The annual pCO_2 cycle for the inner-shelf (top), mid-shelf (middle), and outer-shelf (bottom). The interpolated data, as shown, were used for flux calculations.

months (Table 1, Fig. 5). By late spring, the inner shelf is well above saturation while the mid and outer shelves are near saturation. Levels climb above atmospheric CO_2 between spring and summer over the entire shelf, but by mid-autumn the mid and outer shelves are once again below saturation. The declining amplitude of the annual cycle is clear as one progresses offshore. The outer-shelf is in general closer to atmospheric equilibrium than the inner and mid-shelf regions. Much of the large annual range in pCO_2 can be explained by the annual solar cycle. Because of the shallow shelf water and its relatively long residence time, seasonal heating and cooling dramatically alter the seasonal surface water temperature (e.g. Loder et al., 1998). The inner-shelf temperature varies from $\sim 4^{\circ}C$ to $25^{\circ}C$ (Fig. 2). Over this range, the pCO_2 would drop to $\sim 220\,\mu atm$ during the winter and rise to $\sim 560\,\mu atm$ in the summer, if alkalinity and total CO_2 were to remain constant at $2100\,\mu mol\,kg^{-1}$ and $1903\,\mu mol\,kg^{-1}$, respectively

(using the CO_2 equilibrium program of Lewis and Wallace, 1998). We also have found that upon spring stratification, pCO_2 increased by $\sim 100\,\mu atm$ on the mid-shelf, almost all of which can be explained by surface heating ($\sim$YD 115 in Fig. 3) (DeGrandpre, unpublished). Boehme et al. (1998) found that net community production offsets the effects of heating to some extent, as the increased solar radiation that drives heating is also the primary forcing for photosynthesis. In autumn, there is still sufficient light for significant production, and this, accompanied by increased vertical mixing and cooling, creates undersaturated conditions that are subsequently sustained throughout the winter. As discussed above, local upwelling and freshwater fluxes affect nearshore pCO_2 levels in the short-term, whereas, short-term variability is small (by comparison) in the mid-shelf region as shown by Boehme et al. (1998) and Fig. 3. Like the nearshore water, the outer-shelf is the interface for mixing of different water masses, however, these waters are in general closer to saturation and less variable, reflecting their source waters (Bates and Hansell, 1999).

4.2. Air–sea CO_2 fluxes

As stated above, air–sea CO_2 fluxes were estimated using the Wanninkhof (1992) (W) and Liss and Merlivat (1986) (LM) gas-transfer velocities. The January–March LEO and SAMI Cape Hatteras data (Fig. 3), which were collected at monthly and half-hourly intervals, respectively, are used to examine the sensitivity of the W and LM fluxes to wind and CO_2 undersampling. Wind-speed data are shown in Fig. 6. As recognized in numerous past studies, the W and LM parameterizations predict significantly different fluxes, as much as a factor of 2 difference in this case (Table 2). The W flux is more sensitive to wind speed and CO_2 averaging than the LM flux (Table 2) because of the nonlinear form of the W gas-transfer parameterization. Wind speed temporal averaging has a relatively small effect (up to $\sim 12\%$) compared to the uncertainty in the gas-transfer velocity. Spatially averaging the wind is also a potential source of error, but because the entire MAB has similar wind speeds (Fig. 6), the flux can be calculated using the mean hourly wind speed calculated from the six NDBC buoys. For example, using a local wind speed changes the W flux by only $-0.02\,mol\ C\,m^{-2}\,yr^{-1}$. Averaging the CO_2 data also has little effect on the flux (Table 2). These are mid-shelf data; as discussed above, the inner-shelf would be more sensitive to undersampling pCO_2.

The regional and annual fluxes are presented in Table 3, calculated using the mean hourly

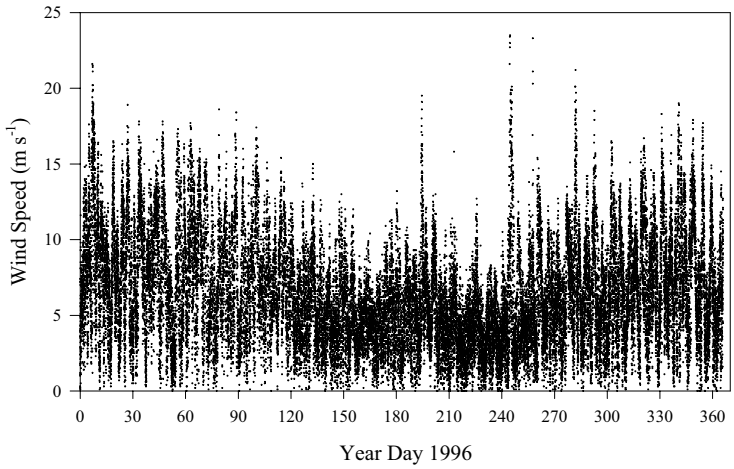

Fig. 6. Wind speed from all six NDBC buoys (Fig. 1) during 1996. Seasonal mean wind speeds during winter, spring, summer, and autumn are 8.0 ± 0.9, 5.5 ± 0.8, 4.9 ± 1.0, and $6.99\pm0.9\,m\,s^{-1}$, respectively. Winds were obtained at different heights above the sea-surface and are not corrected to 10 m height. The hourly mean of all six wind time-series was used for flux calculations.

averaged MAB wind speed and hourly interpolated ΔpCO_2 for each region. All three regions are net sinks for atmospheric CO_2 resulting in a net MAB sink of $\sim 1 \pm 0.6$ Mt C yr^{-1} using the W gas-transfer parameterization. The uncertainty is based on propagation of the uncertainty associated with each regional ΔpCO_2. (Table 3). The data-based uncertainty is probably underestimated because at times there were no data available. Although the inner-shelf flux has a large uncertainty due to undersampling, its surface area is much smaller than the other regions and, as a result, it does not contribute significantly to the overall uncertainty. Additionally, the uncertainty due to the gas-transfer velocity is comparable to the ΔpCO_2 uncertainty. Researchers are continuing to refine our understanding of the processes that control gas-transfer rates (Wanninkhof and McGillis, 1999; Nightingale et al., 2000). When we have greater confidence in K_w, the accuracy of flux estimates such as these can be updated and improved. Additional error arises from uncertainty in the atmospheric CO_2. The atmospheric value is likely higher than 360 ppm on average due to input of continental air. Using 370 ppm, the flux estimate increases by $\sim 40\%$ (Table 3). We have also used multiple years in the analysis so the calculated uncertainty already contains some of the interannual variability. Boehme et al. (1998) found interannual variability of $\sim 35\%$ between 2 years.

Finally, we attempt to address why the MAB is a net sink for atmospheric CO_2. We presented in the Section 1, that, to be a net sink, an ocean margin must fix, export and/or ingas carbon faster than it is remineralized and/or offgased. One interesting possibility is that the MAB could sequester atmospheric CO_2 without net production of organic carbon. Seasonal cooling and heating can result in a net uptake because of asymmetry in the wind speed distribution (Fig. 6). Winds are highest in the winter months, favoring gas exchange during periods when undersaturation is greatest (Table 1). A simple calculation indicates

Table 2
Flux sensitivity to choice of gas transfer velocity parameterization and undersampling of wind and pCO_2

	Averaging interval	W	LM
Wind/pCO_2 averaging (LEO YD 40–130)	Hourly	−7.1/−7.1	−3.9/−3.9
	Daily	−6.9/−7.1	−3.9/−3.9
	Weekly	−6.6/−7.1	−3.9/−3.9
	Monthly	−6.5/−7.1	−3.9/−3.9
Wind/pCO_2 averaging (SAMI Cape Hatteras YD 40–130)	Hourly	−5.4/−5.4	−3.0/−3.0
	Daily	−5.2/−5.4	−2.9/−3.0
	Weekly	−4.9/−5.3	−2.9/−2.9
	Monthly	−4.8/−5.3	−2.9/−2.9

W and LM are the Wanninkhof (1992) and Liss and Merlivat (1986) gas transfer velocities, respectively. Wind and CO_2 data from Figs. 6 and 3 were used. All wind and pCO_2 sensitivity calculations use hourly averaged pCO_2 and wind, respectively (e.g. Daily W data is daily averaged wind with hourly pCO_2 on the left, and on the right is daily averaged pCO_2 with hourly wind). Flux units are mol C m^{-2} yr^{-1}.

Table 3
Regional and entire MAB annual gas fluxes calculated using the ΔpCO_2 data hourly interpolated over an annual cycle and the mean MAB hourly wind speed calculated from the data in Fig. 6

Location	Area (m^2)	Annual flux (mol C m^{-2} yr^{-1})			Net flux (Mt C yr^{-1})	
		W	LM	% uncert.	W	LM
Inner-shelf	7.4×10^9	−0.9	−0.5	±70%	−0.1	0.0
Mid-shelf	32.0×10^9	−1.6	−0.9	±80%	−0.7	−0.5
Outer-shelf	23.7×10^9	−0.7	−0.4	±10%	−0.2	−0.1
Mean MAB flux (360 ppm) (±60%)					−1.0	−0.6
Mean MAB flux (370 ppm) (±60%)					−1.4	−0.8

All fluxes were calculated using 360 ppm atmospheric CO_2. Uncertainties were calculated by propagating the standard deviation of the averaged pCO_2 data only.

that, for an annual heating cycle from 4°C to 25°C with the minimum temperature on 1 January, the W flux would be –1.1 mol C m^{-2} yr^{-1} using the mean wind speed distribution in Fig. 6 (and assuming the ΔpCO_2 is not altered by gas exchange). This flux is similar to the data-based flux (Table 3). If the wind speed were constant at 6.5 m s^{-1}, the system would become a net source with a W flux of +0.44 mol C m^{-2} yr^{-1}! In this simulation, the MAB releases CO_2 because the absolute ΔpCO_2 is greater in the summer, due to the nonlinear dependence of pCO_2 with temperature. If the water remained on the shelf, the water would eventually reach a new saturation level with no net exchange; therefore, water export is required to sustain this flux. The wind-thermodynamic sink can be supplemented by net biological production, which further decreases pCO_2 in the fall and winter and reduces the amplitude of the summer heating maximum (Boehme et al., 1998). The similarity between the data-based fluxes and the thermodynamic flux suggests that net production counterbalances pCO_2 increases due to remineralized terrestrial carbon (e.g. Vodacek et al., 1997), upwelling sources (Glenn et al., 1996), and net heating (Aikman, 1984). The former two fluxes are very difficult to quantify, so the answer to this question will, for the meantime, remain unknown.

4.3. Summary

Data support that there is a net annual uptake of ~1 mol m^{-2} yr^{-1} CO_2 on the MAB resulting in a net uptake of ~1 Mt C yr^{-1}. The flux (mol C m^{-2} y^{-1}) is significantly smaller than that found recently in other ocean margins (Tsunogai et al., 1999; Frankignoulle and Borges, 2001). Although both the East China Sea and Northeastern Atlantic shelf waters warm significantly during summer, neither area experiences the high levels of summer supersaturation (>400 μatm) found on the MAB (see also Kempe and Pegler, 1991; Wang et al., 2000). Spring stratification leads to depletion of nutrients in the surface water on the MAB and carbon cycling approaches steady-state conditions (Sharp and Church, 1981; Falkowski et al., 1983). Consequently, the increase in pCO_2 due to heating is not mitigated by new production in the isolated surface water. In contrast, nutrient standing stocks and summer freshwater sources appear to promote significant summertime new production in the East China Sea and European shelf (e.g. Wang et al., 2000; Frankignoulle et al., 1996). Clearly, the MAB does not follow Tsunogai et al.'s (1999) "continental shelf pump" paradigm and their extrapolation to global fluxes could significantly overestimate the continental shelf sink. Nonetheless, continental shelves, essentially overlooked during past international field studies, appear to play a substantial role in the oceanic uptake of atmospheric CO_2. Further studies such as these will be required in other ocean margins to further constrain the oceanic sink.

Acknowledgements

We are grateful to the many people who contributed to the gathering and analysis of the data used in this study. Special thanks in this regard go out to Dave Chipman, Rose Petrecca, Clare Reimers, Chris Sabine, Sue Boehme, Jeff Kinder, Wade McGillis, Matt Baehr, John Goddard, Taro Takahashi and the Captains and crews of the R.V. *Oceanus* and R.V. *Endeavor*. We also thank NOAA NDBC for their invaluable mooring data. Charlie Flagg, Steve Lorhenz, and Creighton Wirick provided helpful discussions. This work was supported by DOE Grants DE-FG02-92ER61437 and DE-FG03-96ER62224 and NSF Grant OCE-9812513.

References

Aikman, F., 1984. Pycnocline development and its consequences in the Middle Atlantic Bight. Journal of Geophysical Research 89, 685–694.

Bates, N.R., Hansell, D.A., 1999. A high resolution study of surface layer hydrographic and biogeochemical properties between Chesapeake Bay and Bermuda. Marine Chemistry 67, 1–16.

Bates, N.R., Michaels, A.F., Knap, A.H., 1996. Seasonal and interannual variability of oceanic carbon dioxide species at the US JGOFS Bermuda Atlantic time-series study (BATS) site. Deep-Sea Research II 43, 347–383.

Bates, N.R., Takahashi, T., Chipman, D.W., Knapp, A.H., 1998. Variability of pCO_2 on diel to seasonal time scales in the Sargasso Sea. Journal of Geophysical Research 103, 15567–15585.

Biscaye, P.E., Flagg, C.N., Falkowski, P.G., 1994. The shelf edge exchange processes experiment, SEEP-II: an introduction to hypotheses, results and conclusions. Deep-Sea Research II 41, 231–252.

Boehme, S.E., Sabine, C.L., Reimers, C.E., 1998. CO_2 fluxes from a coastal transect: a time-series approach. Marine Chemistry 63, 49–67.

Chipman, D.W., Sutherland, S.C., Takahashi, T., 1995. Determination of ocean/atmosphere carbon dioxide flux within the OMP study area. Final Technical Report for Grant DE-FG02-92ER61451, Lamont–Doherty Observatory of Columbia University, 16 pp.

Churchill, J.H., Cornillon, P.C., 1991. Gulf stream water on the shelf and upper slope north of Cape Hatteras. Continental Shelf Research 11, 409–431.

Codispoti, L.A., Friederich, G.E., Iverson, R.L., Hood, D.W., 1982. Temporal changes in the inorganic carbon system of the southeastern Bering Sea during spring 1980. Nature 296, 242–245.

DeGrandpre, M.D., Reimers, C.E., 2000. Air–sea CO_2 fluxes on the US Middle Atlantic Bight. American Geophysical Union Ocean Sciences National Meeting, Abstract OS11M-11, San Antonio, TX.

DeGrandpre, M.D., Hammar, T.R., Smith, S.P., Sayles, F.L., 1995. In situ measurements of seawater pCO_2. Limnology and Oceanography 40, 969–975.

DeGrandpre, M.D., Hammar, T.R., Wallace, D.W.R., Wirick, C.D., 1997. Simultaneous mooring-based measurements of seawater CO_2 and O_2 off Cape Hatteras, North Carolina. Limnology and Oceanography 42, 21–28.

DeGrandpre, M.D., Baehr, M.M., Hammar, T.R., 1999. Calibration-free optical chemical sensors. Analytical Chemistry 71, 1152–1159.

Falkowski, P.G., Vidal, J., Hopkins, T.S., Rowe, G.T., Whitledge, T.E., Harrison, W.G., 1983. Summer nutrient dynamics in the Middle Atlantic Bight: primary production and utilization of phytoplankton carbon. Journal of Plankton Research 5, 515–537.

Falkowski, P.G., Flagg, C.N., Rowe, G.T., Smith, S.L., Whitledge, T.E., Wirick, C.D., 1988. The fate of a spring phytoplankton bloom: export or oxidation? Continental Shelf Research 8, 457–484.

Frankignoulle, M., Borges, A.V., 2001. European continental shelf as a significant sink for atmospheric carbon dioxide. Global Biogeochemical Cycles 15, 569–576.

Frankignoulle, M., Elskens, M., Biondo, R., Bourge, I., Canon, C., Desgain, S., Dauby, P., 1996. Distribution of inorganic carbon and related parameters in surface seawater of the English Channel during spring 1994. Journal of Marine Systems 7, 427–434.

Glenn, S.M., Crowley, M.F., Haidvogel, D.B., Song, Y.T., 1996. Underwater observatory captures coastal upwelling off New Jersey. EOS Transactions 77, 233–236.

Hoppema, J.M.J., 1991. The seasonal behavior of carbon dioxide and oxygen in the coastal North Sea along the Netherlands. Netherlands Journal of Sea Research 28, 167–179.

Kempe, S., Pegler, K., 1991. Sinks and sources of CO_2 in coastal seas: the north sea. Tellus 43B, 224–235.

Lewis, E., Wallace, D.W.R., 1998. Program developed for CO_2 system calculations. ORNL/CDIAC-105, Carbon Dioxide Information Analysis Center, Oak Ridge National Laboratory, US Department of Energy, Oak Ridge, TN.

Liss, P.S., Merlivat, L., 1986. Air–sea gas exchange rates: introduction and synthesis. In: Buat-Menard, P. (Ed.), The Role of Air–Sea Exchange in Geochemical Cycling, NATO ASI Series C: Mathematical and Physical Sciences, 185, 113–128.

Liu, K.K., Atkinson, L., Chen, C.T.A., Gao, S., Hall, J., Macdonald, R.W., Talaue McManus, L., Quiñones, R., 2000a. Exploring continental margin carbon fluxes on a global scale. EOS Transactions 81, 641–644.

Liu, K.K., Iseki, K., Chao, S.-Y., 2000b. Continental margin carbon fluxes. In: Hanson, R.B., Ducklow, H.W., Field, J.G. (Eds.), The Changing Ocean Carbon Cycle: A midterm synthesis of the Joint Global Ocean Flux Study, International Geosphere–Biosphere Programme Book Series. Cambridge University Press, Cambridge, pp. 187–239.

Loder, J.W., Petrie, B., Gawarkiewicz, G., 1998. The coastal ocean off Northeastern North America: a large-scale view. In: Robinson, A.R., Brink, K.H. (Eds.), The Sea, Vol. 11. Wiley, New York, pp. 105–133.

Münchow, A., Garvine, R.W., 1993. Dynamical properties of a buoyancy-driven coastal current. Journal of Geophysical Research 98, 20063–20077.

Nightingale, P.D., Malin, G., Law, C.S., Watson, A.J., Liss, P.S., Liddicoat, M.I., Boutin, J., Upstill-Goddard, R.C., 2000. In situ evaluation of air–sea gas exchange parameterizations using novel conservative and volatile tracers. Global Biogeochemical Cycles 14, 373–387.

O'Reilly, J.E., Busch, D.A., 1984. Phytoplankton primary production on the northwestern Atlantic Shelf. Rapport et Process-Verbaux des Reunions-Conseil International pour l'Exploration de la Mer 183, 255–268.

Ryan, J.P., Yoder, J.A., Cornillon, P.C., 1999. Enhanced chlorophyll at the shelfbreak of the Mid-Atlantic Bight and Georges Bank during the spring transition. Limnology and Oceanography 44, 1–11.

Sharp, J.H., Church, T.M., 1981. Biochemical modeling in coastal waters of the Middle Atlantic States. Limnology and Oceanography 26, 843–854.

Smith, S.V., Hollibaugh, J.T., 1993. Coastal metabolism and the oceanic organic carbon balance. Review of Geophysics 31, 75–89.

Takahashi, T., Chipman, D.W., Goddard, J., Sutherland, S.C., 2001. Underway pCO_2 measurements in surface waters during the Ocean Margins Program cruises in the northwestern Atlantic Ocean. Final Technical Report for Grant

DE-FG02-95ER62065, Lamont–Doherty Observatory of Columbia University, 16 pp.

Tans, P.P., Fung, I.Y., Takahashi, T., 1990. Observational constraints on the global atmospheric CO_2 budget. Science 247, 1431–1438.

Tsunogai, S., Watanabe, S., Sato, T., 1999. Is there a "continental shelf pump" for the absorption of atmospheric CO_2? Tellus 51B, 701–712.

Vodacek, A., Blough, N.V., DeGrandpre, M.D., Peltzer, E.T., Nelson, R.K., 1997. Seasonal variation of CDOM and DOC in the Middle Atlantic Bight: terrestrial inputs and photo-oxidation. Limnology and Oceanography 42, 674–686.

Wallace, D.W.R., Wirick, C.D., 1992. Large air–sea gas fluxes associated with breaking waves. Nature 356, 694–696.

Wang, S.-L., Chen, C.-T.A., Hong, G.-H., Chung, C.-S., 2000. Carbon dioxide and related parameters in the East China Sea. Continental Shelf Research 20, 525–544.

Wanninkhof, R., 1992. Relationship between wind speed and gas exchange over the ocean. Journal of Geophysical Research 97, 7373–7382.

Wanninkhof, R., McGillis, W.R., 1999. A cubic relationship between air–sea CO_2 exchange and wind speed. Geophysical Research Letters 26, 1889–1892.

Wanninkhof, R., Asher, W., Weppernig, R., Chen, H., Schlosser, P., Langdon, C., Sambrotto, R., 1993. Gas-transfer experiment on Georges Bank using two volatile deliberate tracers. Journal of Geophysical Research 98, 20237–20248.

Weiss, R.F., 1974. Carbon dioxide in water and seawater: The solubility of a non-ideal gas. Marine Chemistry 2, 203–215.

Wirick, C.D., 1994. Exchange of phytoplankton across the continental shelf-slope boundary of the Middle Atlantic Bight during spring 1988. Deep-Sea Research II 41, 391–410.

Wong, C.S., Chan, Y.-H., 1990. Temporal variations in the partial pressure and flux of CO_2 at ocean station P in the subarctic northeast Pacific Ocean. Tellus 43B, 206–223.